

MULTI-RESOURCE INTEGRATION ASSOCIATED WITH THE DEPLOYMENT OF HYDROGEN AND DERIVATIVES IN AN INDUSTRIAL HUB

N'Guessan Charles Tano ^{1,2,3*}, Louis-Marie Malbec ³, Assaad Zoughaib ¹, Solène Le Bourdieu ²

¹ Mines Paris – Université PSL, Centre d'Efficacité Énergétique des Systèmes (CES), Palaiseau, France.

² EDF R&D, Technology and Research for Energy Efficiency, Moret-Loing-et-Orvanne, France.

³ IFP Energies Nouvelles, Economics and Technology Intelligence, Rueil-Malmaison, France.

*Corresponding Author: n-guessan-charles.tano@minesparis.psl.eu

ABSTRACT

The objective of this paper is to propose optimal strategy for the deployment of hydrogen in an industrial hub subject to several constraints and following an eco-industrial park (EIP) scheme. The study was performed using a multi-period MILP model that minimizes the total annualized cost of the overall system. In practice, the attractiveness of an industrial hub regarding the production of Fischer-Tropsch fuels from electrolytic hydrogen and captured carbon dioxide from a nearby steel industry was evaluated. Key results indicate that Fischer-Tropsch (FT) processing plant can be perfectly integrated in industrial hub via the design of EIP. In such scheme, global economic gain due to synthetic fuels sales, heat valorization and economies of scale regarding hydrogen production, can be obtained given an appropriate market price of the commodities. When studying legislation-constrained scenarios, considering the European legislation on the production of renewable fuels of non-biological origin and the current ETS market structure, the benefit of designing such EIP becomes controversial, unless FT fuels are supported on the market by environmental regulation. Biogenic source of carbon dioxide should also be available in quantity. Otherwise, the current announced projects might be called off and other production routes of sustainable fuels might be favored.

1 INTRODUCTION

In the context of global decarbonization of the economy, low-carbon hydrogen and its derivatives such as synthetic fuels are expected to play a significant role, especially in hard-to-abate sectors that cannot be realistically electrified. They include steel, ammonia and methanol industries, hydrocarbon refining, aviation, and heavy-duty transport. Hence, for several years now, multiple deployment strategies for hydrogen have been observed around the world. In the literature, most topic-related studies agree to the fact that the hydrogen economy should be structured around key existing industrial hubs. In (IEA, 2019), the International Energy Agency (IEA) has identified coastal industrial hub as one of the major near-term opportunities to boost the clean hydrogen deployment. In fact, around the world, industrial ports already concentrate existing industries that uses fossil hydrogen. Encouraging these plants to shift to cleaner hydrogen production would drive down overall costs. These large sources of hydrogen supply can also feed other local industrial facilities like steel plants, attract new industries such as synthetic fuel production plants and fuel ships, trucks, and part of the captive fleet of the nearby cities. While such hydrogen deployment will contribute to the economic growth of these regions, it will also bring more challenges regarding resources availability and allocation. With the concept of industrial ecology, sustainable and economically viable resource management could be achieved by developing Eco Industrial Park (EIP). Designing EIP consists of enabling synergies between industrial actors at a local scale. It aims at recovering untapped resources like waste heat or wastewater while exchanging energies and resources between local stakeholders. In this regard, the goal of this paper is to propose optimal designs, following an eco-industrial park scheme, of an industrial hub where a dynamic electrolytic hydrogen deployment associated with synthetic fuel production is envisaged. The literature on hydrogen deployment is rich and fast-growing. Several recent review articles, especially (Li et al., 2019) (Sgarbossa et al., 2022) (Riera et al., 2023), provide insight into the research gaps of this field. Among

the key conclusions, these papers all agree that more attention should be paid to hydrogen-related value chains, raw materials supply system, and recovery of by-products from hydrogen production processes. One way to address these neglected aspects is to adopt multi-material and multi-energy integration approaches, based on mathematical optimization techniques. (Ahmed et al., 2020) adopted such systemic methodology to design an integrated carbon capture utilization and sequestration (CCUS) system. The carbon dioxide processing options considered were methanol, ammonia and urea production plants, including water electrolysis for hydrogen production. (Ibrahim and Al-Mohannadi, 2023) extended this model by incorporating spatial aspect for transportation needs and other echelons of the hydrogen supply chain, such as storage. However, the resulted algorithm developed and used in these works is still limited for supply chain analysis since temporality is neglected. By extending the work of (Ghazouani, 2016), (Wissocq, 2021) developed a generic multi-period model that could be used to analyze the deployment of hydrogen while considering multi-resource integration. The novelty of the present work lies within the adoption of a dynamic multi-resource integration approach to study the attractiveness of an industrial territory for Fischer-Tropsch fuel production while considering some of the European regulations.

2 MATHEMATICAL MODEL DESCRIPTION

The optimization model used, based on the work of (Ghazouani, 2016) and (Wissocq, 2021), takes the form of a mixed integer linear program (MILP) with an economic mono objective function and various equality and inequality constraints, which are not extensively described in this paper. An industrial or urban cluster is described by different objects, representing its resource demand or availability across time periods $t \in T$. The elementary objects and sets are:

- Heat streams ($h \in H_p$), defined by two temperatures T_h^{in} , T_h^{out} and an associated heat power $Q_{h,t}$. From these streams, it is possible to model heat demand (cold stream: $T_h^{in} \leq T_h^{out}$) or waste heat availability (hot stream: $T_h^{in} \geq T_h^{out}$) for example.
- Thermal utilities ($h_u \in H_u$) are heat streams but with a variable power $Q_{h_u,t}$ used to satisfy heat and cooling requirement. They are associated to an operating cost.
- Process sources ($j \in J_p$) are defined by a given mass flow $L_{j,t}$ and a composition $y_{j,k,t}$ in pollutant k . They correspond to resource availability.
- Process sinks ($i \in I_p$) are defined by a given mass flow $G_{i,t}$ and an acceptable composition range $z_{i,k,t}^{min}$, $z_{i,k,t}^{max}$ in pollutant k . They correspond to resource demand.
- Variable sources ($j \in J_v$) are available in a cluster to satisfy process sink requirements. Their mass flow rate $L_{j,t}^v$ are unknown for each time period $t \in T$. They represent the input flow of process units or the purchase of a resource, with an associated cost.
- Variable sinks ($i \in I_v$) are available in a cluster in order to discard resources that cannot be used directly. Their mass flow rate $G_{i,t}^v$ are unknown for each time period $t \in T$. They represent the output flow of process units, the discard, or the sale of a resource with an associated price.

These objects are used for simultaneous heat and mass integration whose equations are based on mass conservation, pinch method, and classic transshipment model. A discretized temperature scale is built, provided by source, sink and thermal stream temperatures and shifted with pinch temperature. Heat exchangers are considered in a parallel configuration and their area are computed, assuming that inlet and outlet temperatures are already known (defined as problem parameters). An illustration is given below for non-isothermal mixing. Based on these elementary objects, more sophisticated systems can be integrated to the model, such as:

- Mass networks ($m \in M_{net}$), allowing resource exchanges between clusters, are modeled as a variable source and a variable sink for each resource which represent respectively the resource provided by the network to the cluster and the resource leaving the cluster and entering in the network. There is no mass accumulation in the network. These are also defined by a specific path connecting the clusters and a variable investment cost, which is a function of the path distance.

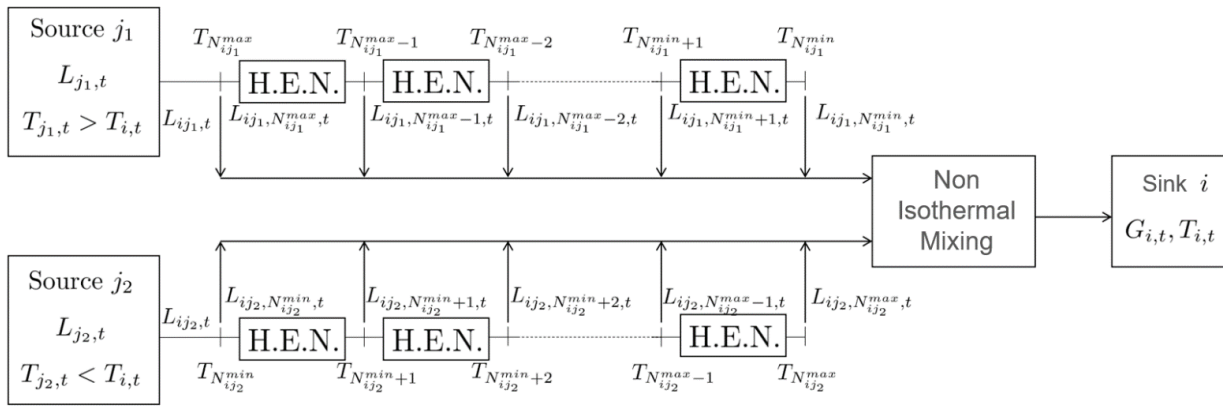


Figure 1: Simplified superstructure for mass and heat integration through non-isothermal mixing (Wissocq, 2021)

- Heat networks ($h_n \in H_{net}$), are modeled by a couple of utilities, representing the hot and cold side of the network. Apart from these, their definition is similar to mass networks.
- Conversion systems ($sc \in SC$) are created by the association of variables sources and sinks and thermal utilities. They are used to model process units or process plants. They are modeled as a grey box system, characterized by efficiency coefficients. Investment and operating costs are associated to these systems.

To avoid computational issues such as problem size, convergence and solving time, a simplified time representation has been introduced. Instead of solving the problem with an hour precision over the whole lifetime, the temporal scale is discretized at three different levels as shown in **Figure 2**. The lifespan is thus reconstituted, with a non-uniform time representation.

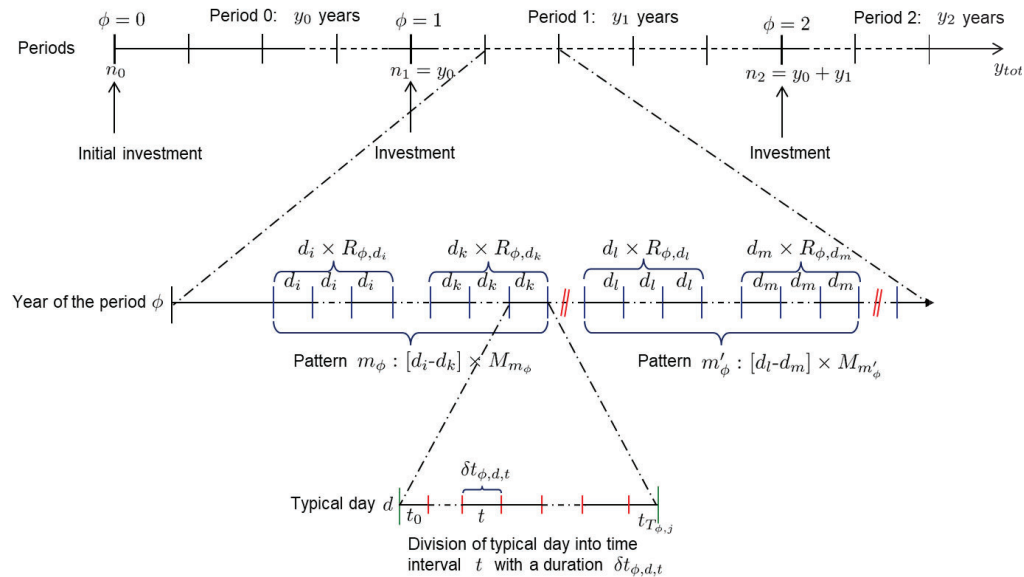


Figure 2: Temporal formulation (Wissocq, 2021)

The objective function is the minimization of total actualized costs (TAC), composed of investment and operating costs:

$$\min TAC = \min \sum_{\phi \in \Phi} \frac{CAPEX_{\phi} + OPEX_{\phi}}{\sum_{y=1}^{N_{op}} (1 + \alpha)^{-y}} \quad (1)$$

$$\forall \phi \in \Phi, CAPEX_{\phi} = \sum_{\phi \in \Phi} \frac{Inv_{\phi}}{(1 + \alpha)^{n_{\phi}}} \quad (2)$$

$$\forall \phi \in \Phi, OPEX_{\phi} = \sum_{y=n_{\phi}+1}^{n_{\phi}+1} \frac{AOC_{\phi}}{(1 + \alpha)^y} \quad (3)$$

$CAPEX_{\phi}$ is the sum of the investment cost Inv_{ϕ} of each period ($\phi \in \Phi$), discounted to the starting year of the period with the actualization ratio α . It includes pipe, conversion system and heat exchanger investment costs, etc. $OPEX_{\phi}$ is the operating cost calculated as the sum of the annual operating cost AOC_{ϕ} of each period discounted to the starting year. It includes purchase of external resources, resources disposal cost, electricity purchase, etc.

Overall, the problem variables to be optimized are the mass flow rates of variable sources and sinks, the network layout, conversion system capacities, the heat utilities loads and heat exchanger network. Binary variables are used to indicate the presence of network edge, conversion system or heat exchanges.

3 CASE STUDY

3.1 Clusters description and territorial layout

The fictive study case described in this section is inspired by a real industrial hub, the Dunkirk industrial port zone which is one of the largest industrial hubs in France. Currently, several industries are implanted in this hub, including an iron and steel manufacturing plant which produces around 6.7 Mt of steel per year in the form of coil and slab. In this study case, this plant will be associated with a hydrogen ecosystem. A life period of 20 years discretized into three periods for dynamic analysis is assumed. The period length was four years, six years, and ten years for period 1, 2 and 3, respectively. At this stage, these phases were not further discretized. As shown in **Figure 3**, this hub is composed of four clusters:

- Cluster A represents a conventional iron and steel manufacturing plant that combines two decarbonization strategies. First, throughout all three phases, part of production is decarbonized by the mean of a carbon capture unit installed for the blast furnace gas. This captured carbon dioxide, with an assumed flowrate of 100 t/h (corresponding approximatively to the production of 7.5 kt/y of crude steel), could either be sequestered with an associated cost of 22 €/tCO₂ (ADEME, 2020), or serve as a feedstock for synthetic fuel production. The second strategy considered is the conversion of part of the remaining plant capacity into a DRI-EAF (Direct Reduction Iron – Electric Arc Furnace) process that uses hydrogen as a reduction agent. This is implemented in period 3 and the estimated hydrogen demand is 2.95 t/h (corresponding approximatively to the production of 370 kt/y of crude steel).
- Cluster B represents the Fischer-Tropsch fuel production plant. The design of this plant highly depends on the available carbon dioxide in the territory.
- Cluster C represents a water electrolysis plant that produces hydrogen for export. The production flow rate is constant at 2 t/h in period 1 and 2 and doubles in period 3.
- Cluster D represents an urban zone with hydrogen demand for a local refueling station. This station is designed to provide hydrogen to a captive heavy-duty fleet starting from year 5 (beginning of period 2). The estimated demand is 0.02 t/h. In addition, residential heat demand for domestic hot water utility is introduced and is limited to 60 MW during the first ten years (periods 1 and 2) and to 80 MW during the remaining years (period 3). An incentive to provide heat to the neighboring city is created by assuming a sale price of 25 €/MWh.

To meet the hydrogen demand, each cluster has the possibility to install an electrolyzer on site or to be supplied from another cluster through hydrogen pipeline¹, which must be constructed. Cluster C is the

¹ Currently, pipelines are the only transportation modes in the model.

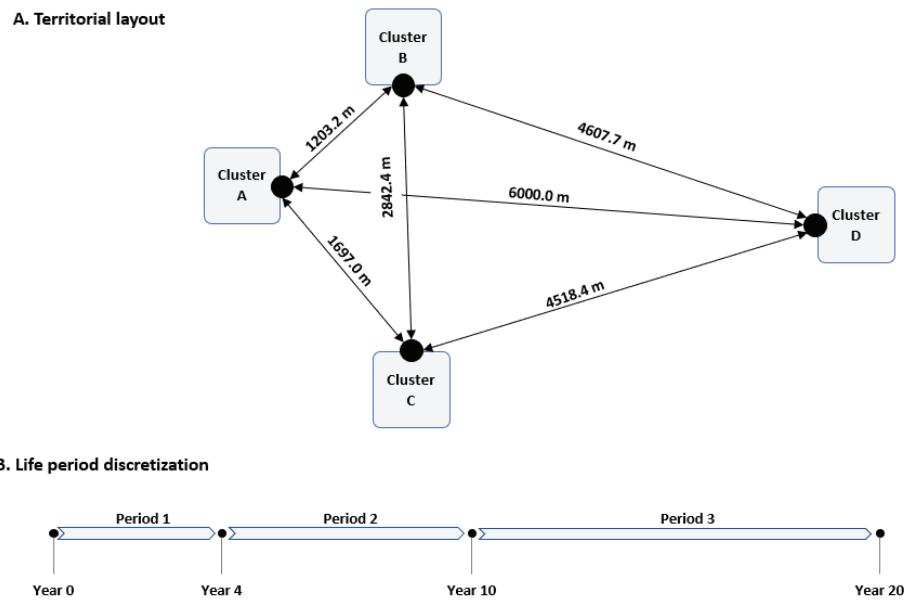


Figure 3: Territorial layout and life period description

only site that can provide hydrogen to the other clusters. Apart from hydrogen, the other resources tracked in this study are carbon dioxide, synthetic fuels, water, electricity, and heat. These resources can be exchanged from one cluster to another one via pipeline according to their needs and availabilities. Electricity and synthetic fuels are the only exceptions. Electricity, coming only from the national grid, is assumed to be available to meet the requirement of the overall hub. When produced, synthetic fuels leave the hub as final product for sales. Moreover, it is assumed that a water network, supplying all four clusters with industrial water, already exists in the industrial hub. Therefore, no investment is required for water pipeline. At this stage, water availability is not limited.

3.2 Process modeling and techno-economic data

In this study, only the alkaline electrolyzers and the FT production plant were explicitly modeled. The carbon capture and DRI-EAF units were not explicitly designed as it is assumed that cluster A is already well integrated and has all the necessary cooling and heating utilities. The modeled processes were considered as grey box technology for mass and heat integration. Their investment costs (CAPEX) were estimated using the “six-tenths rule” to account for economies of scale (Sinnott, 1993). This method is common for rapid cost estimate based on historical data. It consists of using a logarithmic relationship, described by **equation 4**, where C_2 stands for the questioned equipment costs at the scale S_2 (size, capacity, nominal power) of the component, and C_1 and S_1 represent the costs and scale of the known reference component, respectively. n is the scale factor applied to the technology in question.

$$C_2 = C_1 \left(\frac{S_2}{S_1} \right)^n \quad (4)$$

Afterwards, for each of the modeled technologies, this equation was linearized. Two cost components were then obtained: a variable capital cost, representing the cost part that varies according to the technology size, and a fixed capital cost, representing the investment that is independent of the size. Operating cost (OPEX) was estimated by taking into consideration only the feedstock cost and utility cost. Maintenance and labor costs were excluded.

Table 1 shows the resources costs. **Table 2** and **Table 3** summarize the techno-economic data of all the processes. The reference year of 2019 was chosen; thus, all costs were updated to euro (€) 2019. An actualization rate of 5 % was assumed.

Table 1: Commodities costs

Commodities	Price	Sources
Conventional kerosene	600.0 €/t	(Académie des technologies, 2023)
Conventional diesel	674.7 €/t	(Ministère de la Transition Écologique et de la Cohésion des Territoires, 2024)
Conventional naphtha	479.8 €/t	(INSEE, 2024)
Industrial water	0.6 €/t	(Wissocq, 2021)

Table 2: Technical data of the processes

Process		Resources					Sources	
Name	Type	Reference	Input		Output			
Electrolyzer	Alkaline	H ₂	H ₂ O ^A	20.00 t/t _{H₂}	H ₂	1.00 t/t _{H₂}	(H2V, 2019); (Sakas et al., 2022)	
			Electricity	53.57 MWh _e /t _{H₂}	Sensible Heat (80°C→70°C)	20.24 MWh _{th} /t _{H₂}		
Jet fuel production plant	Fischer-Tropsch based process	Kerosene	H ₂	1.36 t/t _{ker}	Kerosene	1.00 t/t _{ker}	(Zang et al., 2021a); (Zang et al., 2021b)	
			CO ₂	14.54 t/t _{ker}	Diesel	0.59 t/t _{ker}		
			Electricity	0.53 MWh _e /t _{ker}	Naphtha	0.55 t/t _{ker}		
					H ₂ O ^B	7.85 t/t _{ker}		
					Latent Heat (100°C)	11.55 MWh _{th} /t _{ker}		
					Sensible Heat (100°C→25°C)	1.61 MWh _{th} /t _{ker}		
		Sensible Heat (75°C→25°C)	0.84 MWh _{th} /t _{ker}					
		Sensible Heat (37°C→28°C)	10.05 MWh _{th} /t _{ker}					
CO₂ capture unit	-	CO ₂	BFG*	-	CO ₂	1.00 t/t _{CO₂}	(Yang et al., 2020)	
			Electricity	1e-3 MWh _e /t _{CO₂}				
DRI-EAF unit	-	Liquid steel	Iron ore	0.60 t/t _{LS}	Liquid steel	1.00 t/t _{LS}	(Vogl et al., 2018); (Bhaskar et al., 2020)	
			H ₂	0.06 t/t _{LS}	H ₂ O ^A	0.48 t/t _{LS}		
			Electricity	0.45 MWh _e /t _{LS}				

* BFG stands for Blast furnace gas

^A Industrial water

^B Treated wastewater, assumed to have the same composition as surface water

Table 3: Economic data of the processes

Process	Investment cost		Additional Operating cost	Sources
	Variable	Fixed		
Electrolyzer				
1-5 MW _e	0.95 M€/MW _e	0.67 M€		(Böhm et al., 2020)
5-1000 MW _e	0.56 M€/MW _e	4.49 M€		
Jet fuel production plant	37.86 M€/t _{TP} .h ⁻¹	86.20 M€		(Zang et al., 2021b)
H₂ pipeline	1500.00 €/m			(RTE and GRTgaz, 2023)
CO₂ pipeline	649.00 €/m			(Joint Research Centre et al., 2011)
Heat (hot water) pipeline	750.00 €/m			(Wissocq, 2021)
CO₂ geologic storage			22.00 €/t _{CO₂}	(ADEME, 2020)
Utility - cooling tower				
10-50 MW _{th}	0.04 M€/MW _{th}	0.59 M€	2.50 €/MW _{th}	(Sinnott, 1993); (Wissocq, 2021)
50-500 MW _{th}	0.02 M€/MW _{th}	2.11 M€	2.50 €/MW _{th}	
Heat exchanger	77.79 €/m ²	5291.90 €		(Wissocq, 2021)

3.3 Results and discussion

Several sub-studies were conducted in this work. These are described below. The corresponding optimization problems were all solved using CPLEX v12.7.1.0 solver on PC (Processor: Intel® Core™ i5-1145G7 @ 2.60GHz– RAM: 8 Go – OS: Windows© 10).

Cooperative governance

This sub-study consists of designing an eco-industrial park in a cooperative scheme involving all the clusters described in **section 3.1**. In cooperative governance, a single actor is assumed to be the owner of the industrial park. Thus, the prices of the resources shared within the hub are not considered in the optimization calculation. Following a preliminary analysis, an electricity cost of 70 €/MWh is assumed, and e-fuels are assumed to be five times more expensive than the conventional fuels. Solving this optimization problem gives the evolution of the industrial hub with the installed capacities and the flowrates of the exchanged resources from year 1 to year 20. To remain concise in the analysis, only the last period, as depicted in **Figure 4**, is discussed below:

- The total captured flow of carbon dioxide is used for synthetic fuel production during the full life period. In fact, as shown above, all the required conditions are met to reach the profitability threshold regarding the plant construction.
- Cluster C fills almost the overall hydrogen needs of the industrial hub as it is more cost effective for the same nominal power to build a larger electrolyzer than multiple small ones. Cluster D is the only exception because it is located too far away. In fact, in this case, the investment cost of a small onsite electrolyzer (1 MW) is lower than the combined investment cost of hydrogen pipeline and the oversizing of the central electrolyzer, despite the economies of scale.
- Cluster B provides heat to cluster D through a newly constructed heat network. By doing so, costs associated to cooling duty is reduced in the synthetic fuel production plant and additional revenues due to heat sales are obtained.
- In cluster D, the electrolyzer heat is also recovered and provided to the neighboring city.

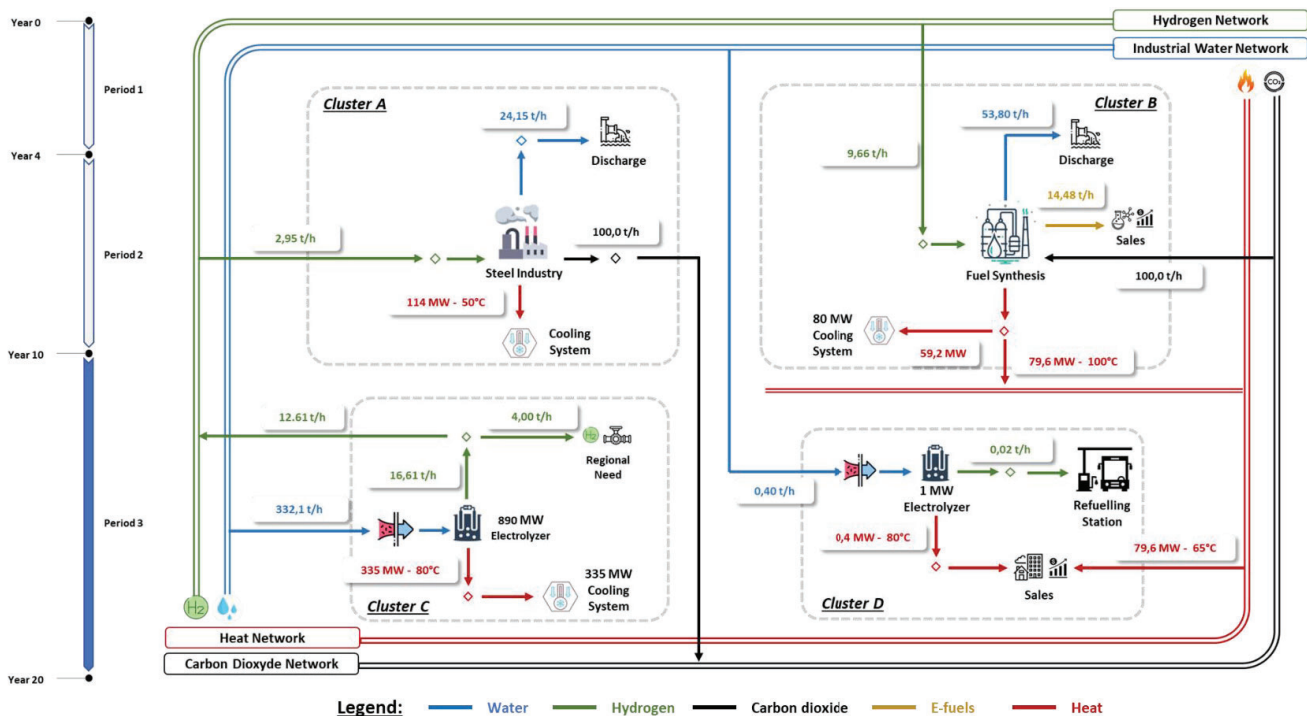


Figure 4: Optimal eco industrial park design (period 3)

As shown in **Figure 5**, the total annualized cost of the overall system is 37% lower with the design of such eco industrial park compared to the reference case, where there is no production of synthetic fuel nor industrial synergy. Most of the gain is due to the production and sales of e-fuels (69 %), and to the recovery and sales of heat to the neighboring (26%). The remaining share comes from economies of scale regarding hydrogen production. Therefore, it is safe to conclude that the economic gain of this industrial park design highly depends on the commodities sales.

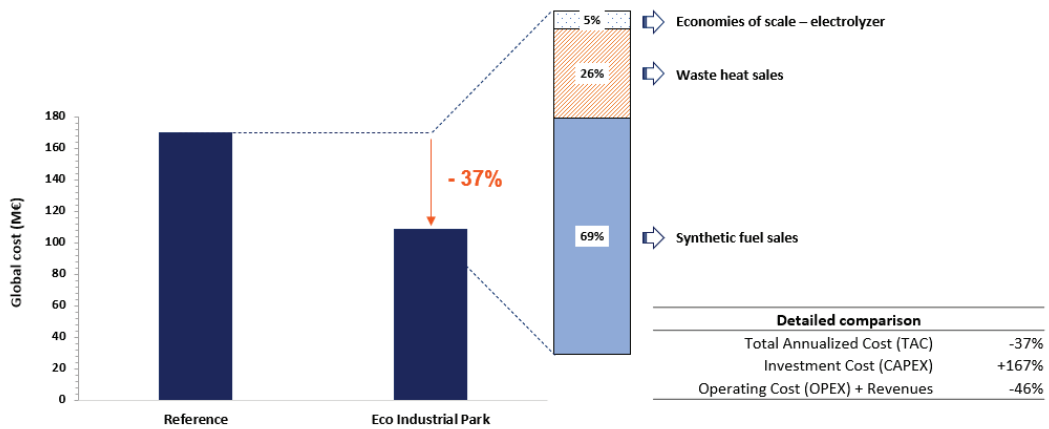


Figure 5: Economic gain related to the eco industrial park design.

Non cooperative governance

As demonstrated earlier, creating an eco-industrial park that integrates e-fuel production is economically viable for the entire industrial hub, assuming the appropriate market price of the commodities. However, a collective economic gain does not guarantee individual benefits since economic divergence may emerge while designing such system. It is therefore crucial to ensure at least a minimum economic profit of each actor for them to join the synergy. This section aims at analyzing the optimal conditions for which the industrial actors participate in the non-cooperative EIP. The approach used here is based on the methodology proposed by (Wissocq, 2021) to design non cooperative industrial park from a cooperative synergy. Only cluster B and C are considered for analysis. Each of these clusters are modeled individually. A third-party actor is introduced to simulate resource demand and availability, with different prices. For a given shared resource, the consumer actor is assumed to be in charge of the transportation cost, thus the pipeline investment expenses. The analysis results of cluster C are depicted in Figure 6 and discussed below.

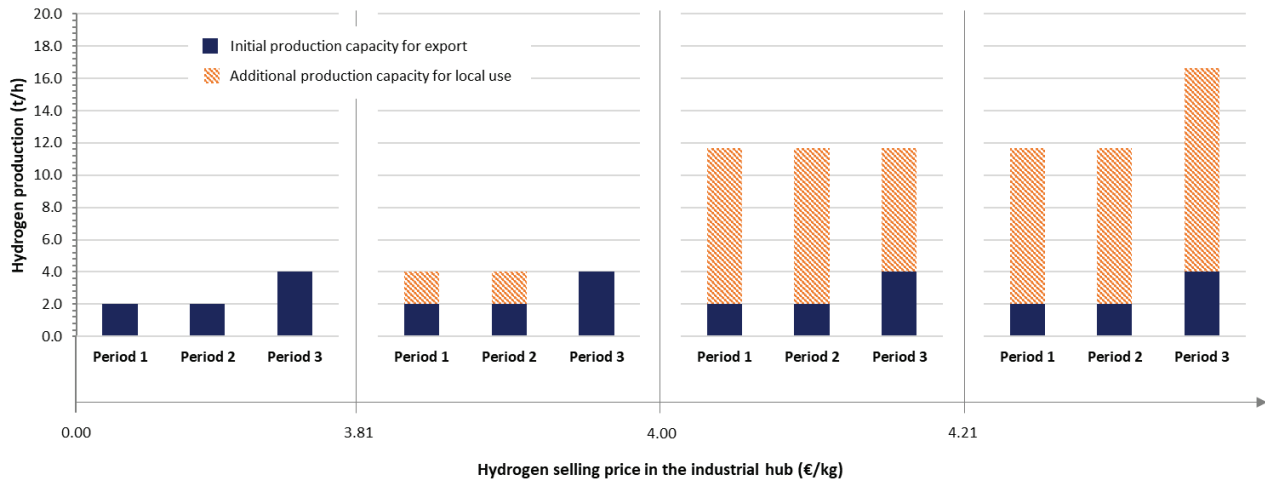


Figure 6: Boundary price conditions of an EIP design involving cluster C.

Several zones, delimited by the selling price of hydrogen in the industrial hub, can be observed:

- For a price below 3.81 €/kg, cluster C does not produce hydrogen for the industrial hub. The initial electrolyzer capacities (for export requirement) are not oversized since the associated additional production costs are not covered when selling hydrogen at this price.

- From 3.81 €/kg to 4 €/kg, cluster C can only deliver 2 t/h of hydrogen during period 1 and 2 to the other actors of the hub. For this price range, the electrolyzer oversizing is limited to the nominal power expected during period 3 to fill the export demand. In fact, cluster C is able to anticipate, from the start, the installation of the capacity required in period 3 because the hydrogen price range is favorable, as opposed to the previous condition discussed.
- From 4 €/kg to 4.21 €/kg, cluster C can provide a constant hydrogen flow of 9.66 t/h to the industrial hub during period 1 and 2. During period 3, while the export demand increases, the installed production capacity remains the same as it is not economical viable to install a new capacity for this price range. Thus, the hydrogen flow provided to the industrial hub is reduced to 7.66 t/h, which does not meet the overall hub demand.
- For cluster C to provide hydrogen to the consuming actors of the industrial hub as observed in the cooperative synergy, a minimum selling price of 4.21 €/kg is required.

Figure 7 illustrates the results of the analysis on cluster B. Hydrogen and carbon dioxide supplies are evaluated for different synthetic fuel price. For this analysis, it is assumed that the maximum cost of carbon dioxide provided by cluster A is 50 €/t. As expected, for a given synthetic fuel price, adjustments to the supply cost of one feedstock must be made when the cost of the other increases. When e-fuels are five times more expensive than the conventional equivalent fuels, the maximum affordable hydrogen price varies between 3.78 €/kg and 4.28 €/kg, depending on the carbon dioxide cost. The previous analysis on cluster C showed that hydrogen must be sold at least at 4.21 €/kg for the latter to fill the hub demand as obtained in the cooperative scheme. Therefore, under these conditions, the equilibrium between bid and offer is obtained when carbon dioxide cost is near zero. If cluster A decides to trade this molecule at a higher price, this will automatically impact the selling price of synthetic fuel.

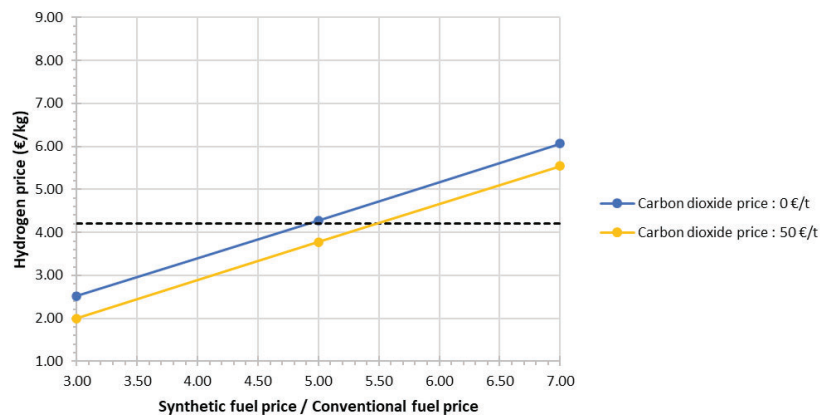


Figure 7: Boundary price conditions of an EIP design involving cluster B.







Legislations constraints consideration

In the Delegated Act from Article 28(5) of the Renewable Energy Directive 2018/2001 ([Commission Delegated Regulation \(EU\) 2023/1185](#)), adopted on February 10, 2023, the European Commission prohibits from 2041 onwards, the use of carbon dioxide stemming from industrial sources to produce renewable fuels of non-biological origin (RFNBOs) and recycled carbon fuels. In fact, the ongoing use of this type of fuels, containing carbon dioxide from non-sustainable source, is incompatible with achieving climate neutrality by 2050 as it would imply the continued use of non-sustainable fuels and thus, the related greenhouse gases emissions. The synthetic fuels produced in this case study fit perfectly into this category and will therefore be affected by the implementation of this regulation. Furthermore, in 2019, the European Commission has published the list of sectors and subsectors deemed at risk of carbon leakage for the period 2021 to 2030 ([Commission Delegated Decision \(EU\) 2019/708](#)). Carbon leakage refers to the situation where industries relocate their production to other countries with less stringent emission regulations due to increasing costs related to climate policies adopted in the initial located area. Since the risk is high in the European union, especially for energy-intensive industries covered by the EU ETS (European Union Emissions Trading System) such as iron and steel

manufacturing facilities, free emission allowances are allocated to safeguard their competitiveness. Therefore, by applying this context to the case study, it may be more profitable for cluster A to sequester its captured carbon dioxide since it can trade its free allowances on the European carbon market, provided that the market price is higher than the storage cost.

The previous sub-studies were conducted by assuming a favorable legislative framework, where fossil carbon dioxide could be used to produce e-fuels and where free emission allowances are not allocated to iron and steel manufacturing facilities. These assumptions limit the analysis done so far since the implementation of the above-mentioned regulations is expected to have a huge impact on the optimal solution. In this sub-section, an attempt to address this limitation is made. Six scenarios, described in **Table 4**, were applied to simulate different conditions that may occur. The objective of this analysis is to evaluate the impacts of these conditions on the investment decision of the synthetic fuel production plant while estimating the maximum price of carbon dioxide from a biogenic source that needs to be used as a replacement of carbon dioxide stemming from cluster A. The key assumptions made are: hydrogen, provided by cluster C, is bought at 4.21 €/kg; Carbon dioxide from a biogenic source is available for the required quantity only after the fossil equivalent is prohibited for e-fuel production; The free emission allowances allocated to cluster A cover its entire greenhouse gas emission.

Table 4: Scenarios description and optimization results

Scenario		Fuel price ratio (synthetic/conventional)	Emission allowances trading price (€/t)	Results	
Name	Regulation			Synthetic fuel production periods	Bio CO ₂ maximum price (€/t)
Scenario 1	End of free emission allowances: Year 4 End of fossil CO ₂ usage for e-fuel production: Year 10	5	40		13
Scenario 2	End of free emission allowances: Year 4 End of fossil CO ₂ usage for e-fuel production: Year 10	5	100		13
Scenario 3	End of free emission allowances: Year 4 End of fossil CO ₂ usage for e-fuel production: Year 10	7	40		188
Scenario 4	End of free emission allowances: Year 4 End of fossil CO ₂ usage for e-fuel production: Year 10	7	100		188
Scenario 5	End of free emission allowances: Year 0 End of fossil CO ₂ usage for e-fuel production: Year 4	5	-		11
Scenario 6	End of free emission allowances: Year 0 End of fossil CO ₂ usage for e-fuel production: Year 4	7	-		188

The results presented in **Table 4** can be interpreted as follows:

- When free emission allowances are allocated to cluster A, the trading price on the ETS market has a significant impact on the investment decision for synthetic fuel production (scenarios 1 and 2). To compensate for the resulting increased cost of carbon dioxide, synthetic fuels must be sold at higher prices (scenarios 3 and 4) during the period in which free allowances are allocated. Otherwise, carbon sequestration pathway is more profitable.
- When fossil carbon dioxide is forbidden, the maximum acceptable supply cost of its biogenic equivalent is directly correlated to the price of the final product. Higher synthetic fuel selling price implies a higher allowable cost threshold for biogenic carbon dioxide.
- The comparison of scenarios 2 and 5 portrays the combined effect of both constraints. In fact, the small decrease of the maximum acceptable price of biogenic carbon dioxide is due to the reduction of the period in which carbon dioxide from cluster A is free. When e-fuels are sold at a higher price, this small change is not noticeable as shown by scenarios 3 and 6.

4 CONCLUSIONS

In this work, multi-resource integration approach was used to study the hydrogen deployment in an industrial hub and the opportunities that can be seized through synthetic fuel production. The results indicate that an EIP, perfectly integrating the Fischer-Tropsch processing plant into the territory, is created when the synthetic fuels are sold at an appropriate price, which is a function of the feedstock cost. This price, however, is always higher than the price of the conventional equivalent fuels. The analysis of the different synergies obtained also shows that heat valorization via heat sale and cooling requirement reduction, as well as economies of scale for hydrogen production, is an economic gain driver. When studying legislation-constrained scenarios, the benefit of designing such EIP becomes controversial. The impact study of the current ETS market structure and the upcoming European legislation regarding the production of RFNBOs draws a clear conclusion. Synthetic fuels will be more expensive than envisaged, which might affect their competitiveness on the market. Biogenic source of carbon dioxide should also be available in quantity. Otherwise, the current announced projects might be called off and other production routes of sustainable fuels might be favored. For future work, water as a key resource in such industrial hub will be integrated. Scenarios including water-stressed periods and more complex territory will be studied. Furthermore, other echelons of the hydrogen supply chain such as hydrogen storage and truck transport will be incorporated.

NOMENCLATURE

Acronyms

BFG	Blast Furnace Gas	$T_{\phi, D_{\phi}}$	Time periods
CCUS	Carbon Capture Utilization and Storage	Φ	Investment periods
DRI	Direct Reduction Iron	C	Clusters
EAF	Electric Arc Furnace	K	Pollutants
EIP	Eco Industrial Park	M	Materials
ETS	Emission Trading System	SC	Conversion system
EU	European Union		
FT	Fischer-Tropsch		
HEN	Heat Exchanger Network		
IEA	International Energy Agency		
MILP	Mixed Integer Linear Programming		
RFNBO	Renewable Fuel of Non-Biological Origin		
TAC	Total Annualized Cost		

Parameters and variables

AOC_{ϕ}	Annual operating cost
$CAPEX_{\phi}$	Sum of the investment cost of each period
G^v	Variable sink mass flow
Inv_{ϕ}	Investment cost of each period
L^p	Variable source mass flow
N_{op}	Number of operating years
$OPEX_{\phi}$	Sum of the annual operating cost of each period
W^{elec}	Electrical power input of conversion system
C	Cost
G	Sink Mass flow
L	Source Mass flow
Q	Utility heat stream power
S	Scale of a component (size, capacity, nominal power)
T	Temperature
y	Year or source pollutant composition
z	Acceptable pollutant composition
α	Actualization ratio

Sets

D_{ϕ}	Typical days
H_{net}	Heat networks
H_p	Process heat streams
H_u	Utility heat streams
I_p	Process sources
I_v	Variable sources
J_p	Process sinks
J_v	Variable sinks
M_{net}	Mass networks

REFERENCES

- Académie des technologies, 2023. La décarbonation du secteur aérien par la production de carburants durables.
- ADEME, 2020. Captage et stockage géologique de CO₂ (CSC) en France. ADEME.
- Ahmed, R., Shehab, S., Al-Mohannadi, D.M., Linke, P., 2020. Synthesis of integrated processing clusters. *Chemical Engineering Science* 227, 115922. <https://doi.org/10.1016/j.ces.2020.115922>
- Bhaskar, A., Assadi, M., Nikpey Somehsaraei, H., 2020. Decarbonization of the Iron and Steel Industry with Direct Reduction of Iron Ore with Green Hydrogen. *Energies* 13, 758. <https://doi.org/10.3390/en13030758>
- Böhm, H., Zauner, A., Rosenfeld, D.C., Tichler, R., 2020. Projecting cost development for future large-scale power-to-gas implementations by scaling effects. *Applied Energy* 264, 114780. <https://doi.org/10.1016/j.apenergy.2020.114780>
- Ghazouani, S., 2016. Modèles linéaires d'optimisation pour la conception simultanée de réseaux de matière et de chaleur d'un éco-parc industriel. Ecole nationale des Mines de Paris - Université PSL.
- Ibrahim, Y., Al-Mohannadi, D.M., 2023. Optimization of low-carbon hydrogen supply chain networks in industrial clusters. *International Journal of Hydrogen Energy* 48, 13325–13342. <https://doi.org/10.1016/j.ijhydene.2022.12.090>
- IEA, 2019. The Future of Hydrogen. International Energy Agency.
- INSEE, 2024. Naphtha (Northwestern Europe) - Spot price - Index in euros - Base 2010 | Insee. URL <https://www.insee.fr/en/statistiques/serie/010002090#Graphique>
- Joint Research Centre, Serpa, J., Morbee, J., Tzimas, E., 2011. Technical and economic characteristics of a CO₂ transmission pipeline infrastructure. Publications Office of the European Union, LU.
- Li, L., Manier, H., Manier, M.-A., 2019. Hydrogen supply chain network design: An optimization-oriented review. *Renewable and Sustainable Energy Reviews* 103, 342–360. <https://doi.org/10.1016/j.rser.2018.12.060>
- Ministère de la Transition Écologique et de la Cohésion des Territoires, 2024. Prix des produits pétroliers. Ministère de la Transition Écologique et de la Cohésion des Territoires. URL <https://www.ecologie.gouv.fr/prix-des-produits-petroliers> (accessed 1.26.24).
- Riera, J.A., Lima, R.M., Knio, O.M., 2023. A review of hydrogen production and supply chain modeling and optimization. *International Journal of Hydrogen Energy*. <https://doi.org/10.1016/j.ijhydene.2022.12.242>
- RTE, GRTgaz, 2023. Enjeux du développement des infrastructures de stockage et de transport d'hydrogène associés au développement de l'électrolyse et leviers d'optimisation avec le système électrique.
- Sakas, G., Ibáñez-Rioja, A., Ruuskanen, V., Kosonen, A., Ahola, J., Bergmann, O., 2022. Dynamic energy and mass balance model for an industrial alkaline water electrolyzer plant process. *International Journal of Hydrogen Energy* 47, 4328–4345. <https://doi.org/10.1016/j.ijhydene.2021.11.126>
- Sgarbossa, F., Arena, S., Tang, O., Peron, M., 2022. Renewable hydrogen supply chains: A planning matrix and an agenda for future research. *International Journal of Production Economics*. <https://doi.org/10.1016/j.ijpe.2022.108674>
- Sinnott, R.K., 1993. CHAPTER 6 - Costing and Project Evaluation, in: Sinnott, R.K. (Ed.), Coulson and Richardson's Chemical Engineering (Second Edition), Chemical Engineering Technical Series. Pergamon, Amsterdam, pp. 209–244. <https://doi.org/10.1016/B978-0-08-041865-0.50014-3>
- Vogl, V., Åhman, M., Nilsson, L.J., 2018. Assessment of hydrogen direct reduction for fossil-free steelmaking. *Journal of Cleaner Production* 203, 736–745. <https://doi.org/10.1016/j.jclepro.2018.08.279>
- Wissocq, T., 2021. Méthodes d'optimisation pour la conception d'éco-pares industriels en considération de la dynamique temporelle. Ecole nationale des Mines de Paris - Université PSL.
- Yang, G., Jiang, Y., You, S., 2020. Planning and operation of a hydrogen supply chain network based on the off-grid wind-hydrogen coupling system. *International Journal of Hydrogen Energy* 45, 20721–20739. <https://doi.org/10.1016/j.ijhydene.2020.05.207>
- Zang, G., Sun, P., Elgowainy, A., Bafana, A., Wang, M., 2021a. Life Cycle Analysis of Electrofuels: Fischer–Tropsch Fuel Production from Hydrogen and Corn Ethanol Byproduct CO₂. *Environmental Science and Technology* 55. <https://doi.org/10.1021/acs.est.0c05893>
- Zang, G., Sun, P., Elgowainy, A.A., Bafana, A., Wang, M., 2021b. Performance and cost analysis of liquid fuel production from H₂ and CO₂ based on the Fischer–Tropsch process. *Journal of CO₂ Utilization* 46, 101459. <https://doi.org/10.1016/j.jcou.2021.101459>